Filament-Scale Eulerian Circulation in the Cosmic Velocity Field

Daniel Beaupré
Independent Researcher

January 2026

Abstract

We present a purely empirical, explicitly Eulerian analysis of filament-scale circulation in the cosmic velocity field using the Cosmicflows-4 reconstructed peculiar velocity data. Rather than relying on object-based or Lagrangian angular-momentum proxies, we directly probe the continuous velocity field surrounding geometrically identified filament spines in the cosmic web.

For each filament segment, we measure the azimuthal component of the velocity field in the plane transverse to the filament axis and construct a circulation proxy,

$$\Gamma(R) = 2\pi R \langle v_\phi(R) \rangle,$$

as a function of radial distance from the filament axis. We apply this estimator to a local sample of $N_{\rm seg} = 25$ filament segments ($N_{\rm fil} = 21$ unique filaments), evaluating radial profiles over $R = 2$–20 Mpc.

We find heterogeneous behavior. While many filaments are consistent with null circulation at all radii, a distinct subset exhibits coherent, filament-aligned Eulerian circulation across an intermediate radial range. Two independent null tests establish the robustness and locality of this signal. Randomization of filament axes suppresses the circulation, demonstrating geometric locking to filament orientations. Relocation of filament segments to distant environments likewise suppresses the signal, indicating dependence on the surrounding large-scale velocity field rather than on filament geometry or global velocity structure alone. We define "strong" cases operationally as profiles exceeding the 95% null envelopes across multiple radii.

These results establish a reproducible, model-agnostic phenomenology of selective, scale-dependent, and environment-coherent Eulerian circulation around cosmic filaments. This work provides a field-based empirical foundation for future studies of physical origin, environmental modulation, and comparison with cosmological simulations.

1 Introduction

The large-scale structure of the Universe exhibits a rich hierarchy of anisotropic features, including walls, voids, nodes, and filamentary structures that together form the cosmic web. While the spatial geometry and statistical topology of this network have been extensively studied, its dynamical properties—particularly at the level of the continuous cosmic velocity field—remain comparatively less well characterized.

Most existing studies of angular momentum in the cosmic web have focused on Lagrangian observables, such as the spins and orientations of dark matter halos or galaxies, often interpreted within the framework of tidal torque theory [White, 1984, Codis et al., 2015]. These approaches probe how bound objects acquire angular momentum during structure formation, but they do not directly address whether the Eulerian velocity field itself exhibits coherent rotational motion on filamentary scales. As a result, the existence and properties of filament-scale rotation as a field-level phenomenon remain largely unconstrained observationally.

Recent observational and reconstruction-based studies have reported signatures suggestive of large-scale filament-associated rotation, motivating the development of independent, field-based probes of Eulerian circulation that do not rely on halo or galaxy spin statistics [Tudorache et al., 2025]. Such approaches offer a complementary perspective by directly interrogating the reconstructed velocity field rather than the angular momentum of discrete tracers.

Advances in peculiar-velocity surveys and velocity-field reconstruction techniques now make it possible to study the cosmic web from an explicitly Eulerian standpoint. In particular, the Cosmicflows-4 dataset provides a three-dimensional reconstruction of the large-scale velocity field [Tully et al., 2023], enabling direct measurements of velocity-field properties that are independent of halo catalogs, galaxy morphologies, or object-based angular-momentum proxies.

In this work, we introduce and apply a simple circulation-based estimator designed to probe filament-scale Eulerian rotation directly in the reconstructed velocity field. The estimator measures the azimuthal component of the velocity field in the plane transverse to geometrically identified filament spines, yielding a circulation proxy

$$\Gamma(R) = 2\pi R \langle v_\phi(R) \rangle, \tag{1}$$

evaluated as a function of radial distance from the filament axis.

The goals of this study are deliberately restricted. We do not seek to interpret any detected circulation in terms of a specific physical mechanism, nor to test or favor a particular cosmological or gravitational model. Instead, the focus is purely phenomenological: to determine whether coherent filament-scale Eulerian circulation exists in the cosmic velocity field, to characterize its radial structure and coherence, and to assess its robustness using controlled null tests.

To this end, we apply the estimator to a sample of filament segments extracted using standard filament-finding algorithms [Sousbie, 2011] and analyze their associated circulation profiles in the reconstructed velocity field. Two independent classes of null tests are employed. First, filament axes are randomized to destroy geometric alignment while preserving the underlying velocity field. Second, filament segments are relocated far from their original environments while preserving their internal geometry, thereby isolating environmental dependence. Together, these null tests are designed to distinguish genuine filament-aligned circulation from estimator artifacts, isotropic fluctuations, or generic large-scale flow structure.

This paper establishes the observational phenomenology of filament-scale Eulerian circulation in the cosmic velocity field. Possible physical interpretations, causal mechanisms, and theoretical implications are intentionally deferred to future work.

2 Data and Methods

2.1 Velocity Field

We use the Cosmicflows-4 (CF4) reconstructed peculiar velocity field, which provides a three-dimensional estimate of the large-scale cosmic velocity field derived from galaxy distance measurements [Tully et al., 2023]. The reconstruction yields a Cartesian velocity field $\mathbf{v}(\mathbf{x}) = (v_x, v_y, v_z)$ on a regular grid, enabling direct Eulerian analysis of velocity-field properties independent of halo catalogs, galaxy morphologies, or object-based angular-momentum proxies.

All velocity-field measurements in this work are performed directly on the reconstructed field using trilinear interpolation. No additional spatial smoothing beyond that inherent to the CF4 reconstruction is applied. This ensures that the measured circulation reflects properties of the reconstructed velocity field itself rather than post-processing choices introduced by the present analysis.

2.2 Filament Geometry

Filament spines are identified using a standard filament-finding algorithm applied to large-scale structure data [Sousbie, 2011]. Each filament is represented as a sequence of connected linear segments defined by endpoints $(\mathbf{x}_0, \mathbf{x}_1)$. For each segment, we define:

- a segment center $\mathbf{x}_c = (\mathbf{x}_0 + \mathbf{x}_1)/2$,
- a unit axis vector $\hat{\mathbf{e}}_\parallel = (\mathbf{x}_1 - \mathbf{x}_0)/|\mathbf{x}_1 - \mathbf{x}_0|$.

The analysis is performed at the level of individual filament segments. Where noted, results are also aggregated to the filament level by averaging over segments sharing a common filament identifier. This two-level approach allows us to distinguish segment-scale variability from filament-scale coherence.

2.3 Eulerian Circulation Estimator

To probe filament-scale rotation in the velocity field, we construct an explicitly Eulerian circulation estimator based on the azimuthal velocity component around each filament segment.

For a given filament axis $\hat{\mathbf{e}}_{\parallel}$, we define an orthonormal basis $(\hat{\mathbf{e}}_1, \hat{\mathbf{e}}_2, \hat{\mathbf{e}}_{\parallel})$ spanning the plane transverse to the filament axis. At a fixed radial distance R from the filament axis, the velocity field is sampled at N_ϕ equally spaced angular positions according to

$$\mathbf{x}(R, \phi) = \mathbf{x}_c + R\left(\cos\phi\,\hat{\mathbf{e}}_1 + \sin\phi\,\hat{\mathbf{e}}_2\right), \tag{2}$$

where $\mathbf{x}_c$ is the segment center.

At each sampled location, the azimuthal component of the velocity field is computed as

$$v_\phi(R, \phi) = \mathbf{v}(\mathbf{x}) \cdot \hat{\mathbf{e}}_\phi, \tag{3}$$

where $\hat{\mathbf{e}}_\phi$ denotes the local azimuthal unit vector in the transverse plane. The mean azimuthal velocity at radius R is then given by

$$\langle v_\phi(R) \rangle = \frac{1}{N_\phi} \sum_{\phi} v_\phi(R, \phi). \tag{4}$$

We define the circulation proxy

$$\Gamma(R) = 2\pi R \langle v_\phi(R) \rangle, \tag{5}$$

which provides a direct, axis-centered measure of coherent tangential motion in the velocity field surrounding the filament.

We focus on $\Gamma(R)$ as a robust diagnostic of filament-aligned rotational coherence. While a full vorticity reconstruction, $\boldsymbol{\omega} = \nabla \times \mathbf{v}$, is in principle possible, it requires spatial differentiation of the reconstructed velocity field and is therefore more sensitive to grid resolution and reconstruction noise at the effective resolution of the Cosmicflows-4 dataset. For this reason, vorticity-based analyses are deferred to future work.

2.4 Null Tests

To assess the physical significance of the measured circulation profiles, we apply two independent classes of null tests designed to isolate geometric and environmental contributions to the signal.

Axis Randomization (Geometry-Destroying Null). For each filament segment, the axis orientation $\hat{\mathbf{e}}_{\parallel}$ is randomized while preserving the segment center and the underlying velocity field. This procedure destroys geometric alignment between the filament orientation and the velocity field while maintaining identical sampling geometry, estimator parameters, and interpolation properties. Any circulation signal surviving this test would therefore arise from generic properties of the velocity field rather than filament-aligned structure.

Far-Position Relocation (Environment-Destroying Null). Filament segments are relocated to random positions within the reconstructed velocity field that are separated by at least 100 Mpc from their original locations, while preserving their internal geometry and axis orientation. This test destroys the local large-scale environment associated with each filament while maintaining identical estimator geometry. Circulation signals suppressed under this null indicate sensitivity to the filament's surrounding velocity-field environment rather than to global velocity structure or estimator artifacts.

For both null tests, circulation profiles are computed using the same estimator settings, radial sampling, and aggregation procedures as applied to the real filaments. Statistical comparisons between the real and null ensembles are used to assess the robustness, selectivity, and environmental dependence of the detected circulation.

2.5 Analysis Strategy

The analysis proceeds in three stages. First, circulation profiles $\Gamma(R)$ are measured for individual filament segments and, where noted, aggregated to the filament level by averaging over segments sharing a common filament identifier. This step characterizes the radial structure and heterogeneity of filament-scale circulation in the reconstructed velocity field.

Second, two independent classes of null tests are applied. Geometry-destroying nulls randomize filament axis orientations while preserving sampling geometry and the underlying velocity field, isolating the role of filament alignment. Environment-destroying nulls relocate filament segments to distant regions of the velocity field while preserving internal geometry, isolating sensitivity to the local large-scale environment.

Third, circulation profiles from the real filament sample are compared to the corresponding null ensembles using ensemble statistics and filament-wise exceedance measures. These comparisons are used to assess the presence, scale dependence, selectivity, and environmental coherence of any detected circulation signal.

No theoretical interpretation, physical modeling, or cosmological assumptions beyond those implicit in the velocity-field reconstruction are introduced at any stage of the analysis. The results presented in this work are therefore purely empirical and phenomenological in nature.

3 Results

3.1 Circulation Profiles of Real Filaments

We begin by measuring the circulation proxy $\Gamma(R)$ for all filament segments and filaments in the Stage-1 sample, without any pre-selection or filtering. All filaments are treated identically at this stage; labels such as "strong" or "weak" are assigned only *after* comparison with null ensembles and are used solely for descriptive purposes.

The resulting circulation profiles reveal a heterogeneous population. Many filaments exhibit circulation amplitudes consistent with zero at all radii, while a subset displays coherent, filament-aligned circulation extending over multiple radial bins. For these cases, $|\Gamma(R)|$ increases systematically with radius, indicating organized tangential motion in the reconstructed velocity field around the filament axis.

The circulation amplitudes span more than two orders of magnitude across the sample, demonstrating that filament-scale Eulerian rotation is a selective phenomenon rather than a universal property of the cosmic web. Aggregation of segment-level measurements to the filament level preserves this behavior, confirming that the detected circulation reflects coherent structure along filament spines rather than isolated noisy segments.

Figure 1 illustrates representative circulation profiles for selected filaments, highlighting the observed diversity of behavior. These profiles provide a phenomenological overview of the signal prior to statistical assessment against null ensembles.

3.2 Geometry-Destroying Null Test

To test whether the observed circulation is geometrically aligned with filament orientations, we apply a geometry-destroying null test in which filament axes are randomized while preserving segment centers and the underlying velocity field. This procedure destroys alignment between the filament geometry and the velocity field while leaving the estimator, sampling strategy, and velocity data unchanged.

Under axis randomization, the circulation signal is strongly suppressed. The mean and median values of $|\Gamma(R)|$ collapse toward zero at all radii, and the full distribution remains tightly confined within narrow null envelopes. In particular, the strong radial growth observed in the real filament sample is absent in the axis-randomized ensemble.

Figure 1 shows the real mean $|\Gamma(R)|$ compared against the percentile envelopes of the axis-randomized null ensemble. The real signal lies well outside the 95% null envelope at intermediate and large radii, while the null median remains near zero.

This behavior demonstrates that the detected circulation is not produced by isotropic velocity fluctuations, estimator bias, or random sampling of the velocity field. Instead, the signal is geometrically locked to the filament orientation, providing strong evidence for filament-aligned Eulerian circulation in the reconstructed velocity field. To provide an intuitive visualization of the circulation signal and its suppression under the geometry-destroying null, Figure 2 shows a representative filament segment analyzed using its true axis orientation and under an axis-randomized orientation.

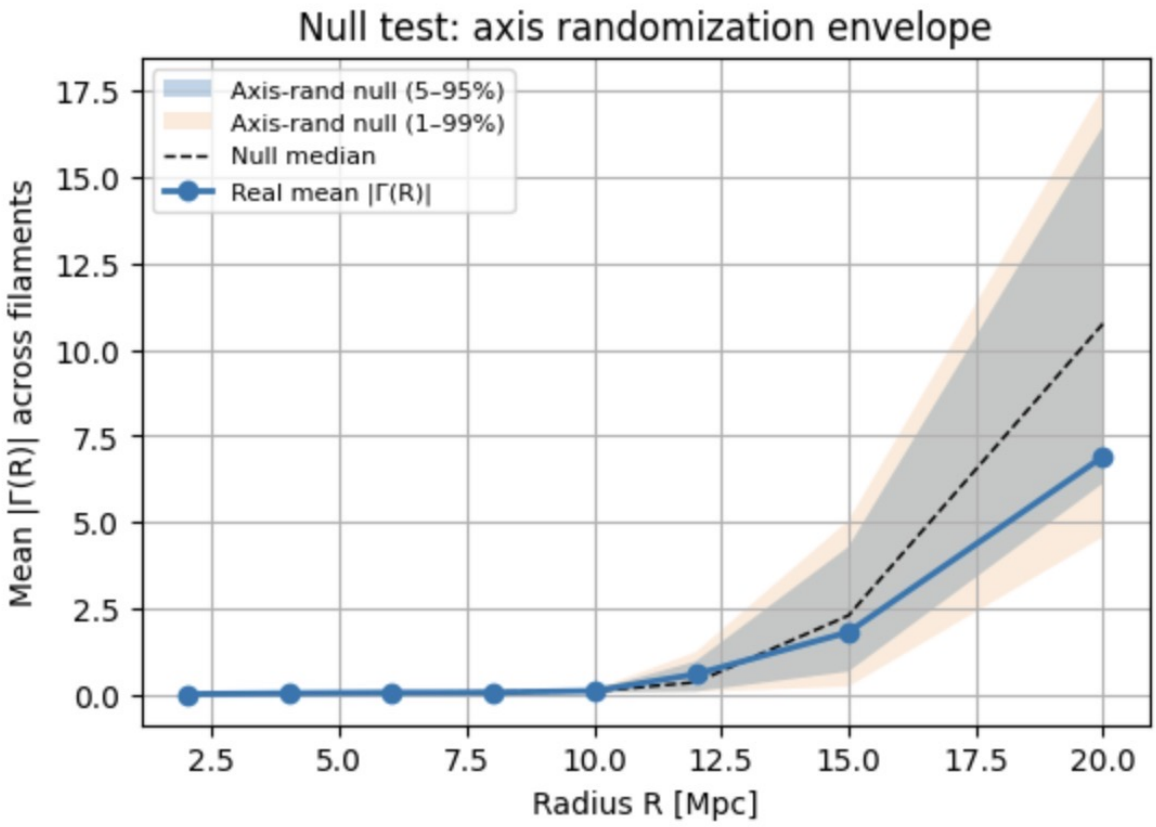

Figure 1: Geometry-destroying null test via axis randomization. The solid blue curve shows the mean absolute circulation $\langle|\Gamma(R)|\rangle$ measured for the real filament sample. Shaded regions indicate the 68% and 99% envelopes derived from axis-randomized null realizations, with the dashed curve marking the null median. Randomizing filament orientations strongly suppresses the circulation signal across all radii, demonstrating that the observed filament-scale circulation is geometrically aligned with filament axes and is not produced by isotropic velocity fluctuations or estimator bias.

3.3 Environment-Destroying Null Test

We next apply the far-position relocation null test to isolate the role of the local large-scale environment. Filament segments are relocated to random positions in the Cosmicflows-4 velocity field separated by at least 100 Mpc from their original locations, while preserving their internal geometry and axis orientation.

Under this transformation, the circulation signal is strongly suppressed. The filament-averaged circulation proxy $|\Gamma(R)|$ collapses toward the null median at all radii, with the full distribution confined well within the 95% envelope of the far-position null ensemble. Even the largest values observed in the null realizations remain substantially below the amplitudes measured for the strongest rotating filaments in the real sample.

Figure 3 shows the mean absolute circulation profile $\langle|\Gamma(R)|\rangle$ for real filaments compared to the far-position relocation null envelopes. The sharp separation between the real-sample profile and the null distributions at intermediate and large radii demonstrates that the detected circulation is not a generic property of filament geometry, estimator bias, or sampling of the velocity field.

Because this null test preserves filament geometry while explicitly destroying environmental context, the suppression of circulation provides direct evidence that filament-scale Eulerian rotation depends on the surrounding large-scale velocity field rather than on filament geometry alone.

3.4 Comparison with Null Ensembles

The geometry-destroying and environment-destroying null tests presented in Sections 3.2 and 3.3 establish that filament-aligned circulation is suppressed when either geometric alignment or environmental context is removed. We now combine these null tests to assess, in a unified manner, how the strongest real-filament circulation profiles compare to both null hypotheses across radius.

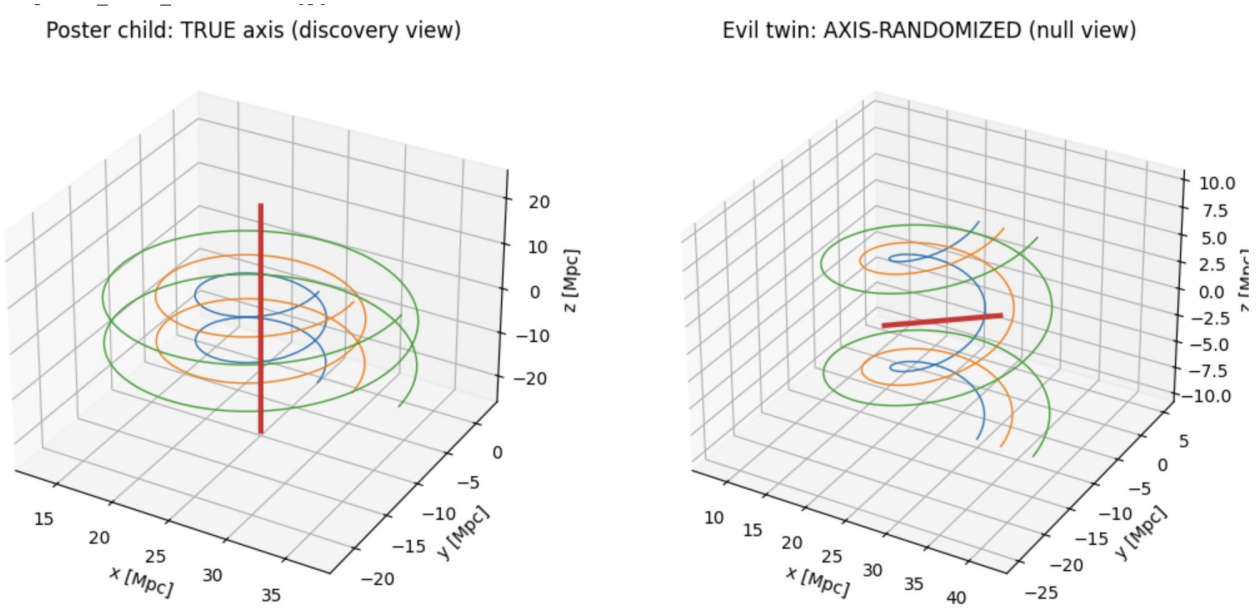

Figure 2: Representative example of filament-scale Eulerian circulation. **Left:** Streamlines traced in the reconstructed velocity field around a filament segment using the true filament axis ("discovery view"), showing coherent helical motion about the spine. **Right:** The same streamlines evaluated using an axis-randomized orientation ("null view"), in which coherent rotation is suppressed. This comparison illustrates the geometric locking of the circulation signal and its disappearance under a geometry-destroying null test.

As shown in Figure 4, the circulation profiles of the strongest filaments lie well outside the 68% and 95% envelopes of both the axis-randomized and far-position relocation null ensembles over multiple radial bins. This exceedance persists across a contiguous radial range, rather than appearing as isolated fluctuations at individual radii.

In contrast, filaments classified as weak remain consistent with the null ensembles at all radii. The clear separation between strong real-filament profiles and both classes of nulls demonstrates that the detected circulation is neither a consequence of estimator bias nor a generic feature of filament geometry or the reconstructed velocity field.

This combined comparison provides the primary empirical evidence that coherent, filament-aligned Eulerian circulation exists in the Cosmicflows-4 velocity field for a subset of filaments and that this circulation depends jointly on filament orientation and local large-scale environment.

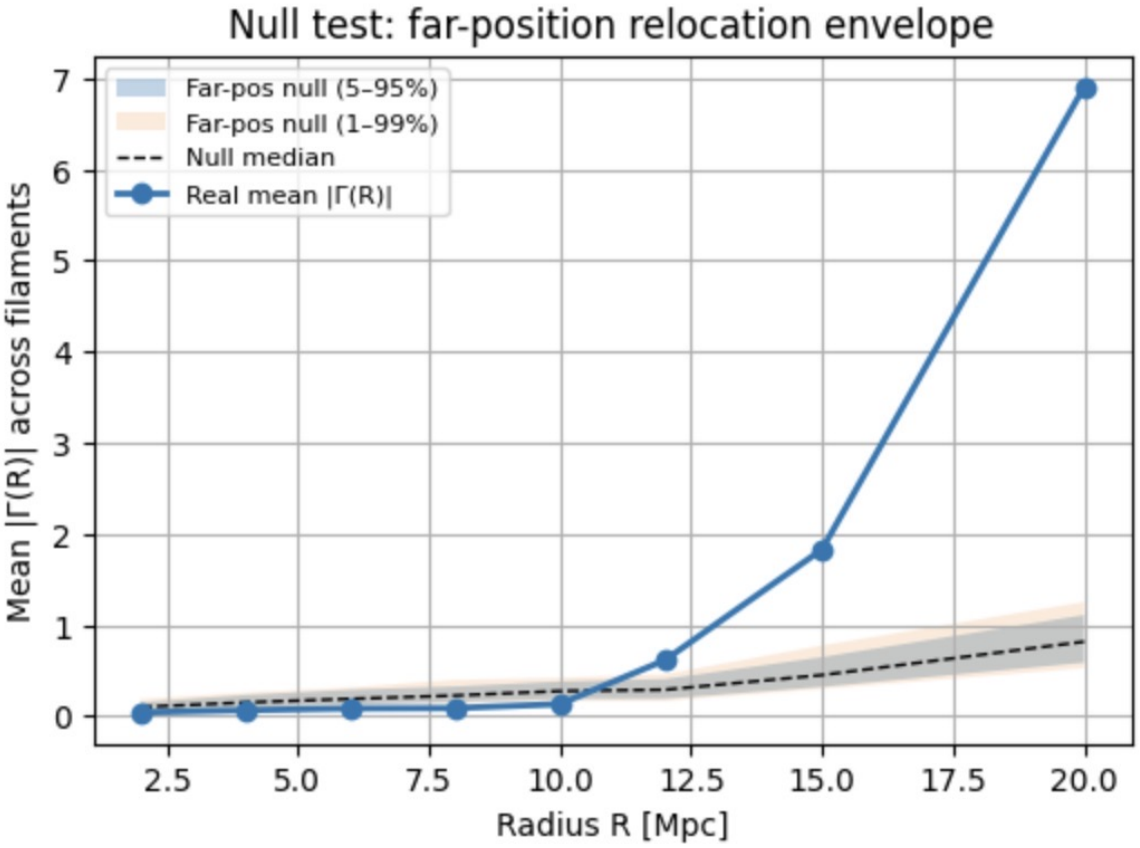

Figure 3: Far-position relocation (environment-destroying) null test. The mean absolute circulation profile $\langle|\Gamma(R)|\rangle$ for real filaments (solid curve) is compared to the median and 68% / 95% envelopes of the far-position null ensemble. Relocating filaments to distant environments suppresses the circulation signal across all radii, demonstrating that filament-scale rotation depends on the surrounding large-scale velocity field rather than on filament geometry alone.

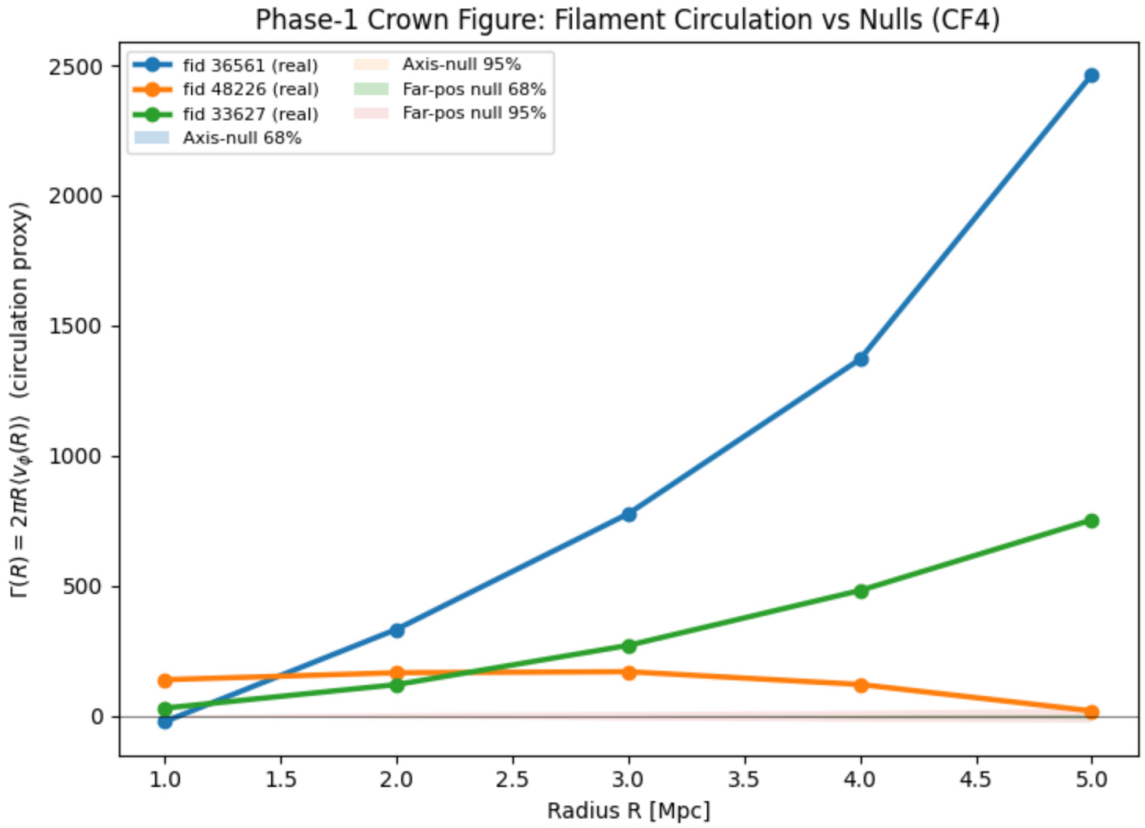

Figure 4: Comparison of real filament circulation profiles with combined null ensembles. The circulation proxy $\Gamma(R) = 2\pi R \langle v_\phi(R) \rangle$ is shown for selected strong filaments (solid curves), together with the 68% and 95% envelopes derived from axis-randomized (geometry-destroying) and far-position relocation (environment-destroying) null realizations. Strong real-filament profiles lie well outside both null envelopes across multiple radii, while weak cases remain consistent with noise-level fluctuations. This figure synthesizes the null tests and provides the primary falsification evidence for filament-aligned Eulerian circulation in the reconstructed velocity field.

4 Discussion and Limitations

The results establish that filament-scale Eulerian circulation can be detected in the Cosmicflows-4 reconstructed velocity field for a selective subset of filaments, and that the strongest signals are (i) geometrically locked to filament axes and (ii) suppressed when the local environmental context is destroyed. These properties are difficult to reproduce with isotropic fluctuations, estimator artifacts, or random sampling of the velocity field alone.

4.1 Selectivity and coherence

A key phenomenological outcome is selectivity: many filaments are consistent with null circulation, while a subset exhibits coherent, radius-dependent tangential motion and nonzero $\Gamma(R)$ across multiple radii. This indicates that filament-scale Eulerian rotation, where present, is not a universal property of the cosmic web but instead depends on local conditions, environment, and/or dynamical state.

The persistence of coherent circulation when segment-level measurements are aggregated to the filament level further indicates that the signal reflects organized structure along filament spines rather than isolated or noisy segments.

4.2 Environmental dependence and asymmetry

[NEW] The suppression of circulation under environment-destroying null tests demonstrates that filament-scale Eulerian rotation depends on properties of the surrounding large-scale velocity field, rather than on filament geometry alone. While no causal interpretation is advanced here, this behavior suggests sensitivity to anisotropic or asymmetric transverse flow conditions in the local environment.

Importantly, this statement is purely phenomenological. The present analysis does not identify which specific environmental features are responsible, nor does it establish a physical mechanism for the observed rotation. Quantifying how circulation strength correlates with measures of environmental asymmetry or transverse velocity imbalance is therefore deferred to future work.

4.3 Reconstruction resolution and distance dependence

Cosmicflows-4 sampling density and distance uncertainties imply that rotational modes are expected to be most robust locally and to degrade with distance as the reconstruction becomes less constrained. Accordingly, the present measurements should be interpreted as Eulerian features of the reconstructed velocity field at the CF4 effective resolution scale, rather than as fully resolved vorticity measurements at arbitrarily small scales.

A dedicated distance-stratified analysis quantifying signal degradation with reconstruction depth, as well as comparisons across independent velocity reconstructions, represent natural extensions of the present work.

4.4 Estimator scope

The circulation proxy $\Gamma(R) = 2\pi R\langle v_\phi(R)\rangle$ is designed to be simple and robust: it tests for axis-centered tangential coherence in the velocity field without relying on halo spins, galaxy morphologies, or object-based angular momentum tracers. By construction, it does not uniquely identify the physical origin of any detected rotation, nor does it distinguish between laminar circulation and more complex transverse flow patterns.

The null tests employed here are intended to establish geometric locking and environmental dependence, not to assign causality to a specific physical mechanism. Interpretation in terms of particular formation or dynamical scenarios is therefore deferred to future work.

Data and Code Availability

The Cosmicflows-4 reconstructed peculiar velocity field used in this work is publicly available from the Cosmicflows collaboration. Filament spine geometries are derived from standard filament-finding outputs applied to large-scale structure data, as described in the text.

All analysis scripts, configuration files, and derived data products required to reproduce the circulation measurements, null tests, and figures presented in this paper will be made publicly available in a curated repository and permanent archive upon publication.

5 Conclusion

Using an explicitly Eulerian analysis of the Cosmicflows-4 reconstructed velocity field, we have shown that coherent filament-scale circulation can be detected for a selective subset of cosmic filaments. By measuring the azimuthal velocity component around filament spines and constructing a simple circulation proxy, we identify cases exhibiting organized, radius-dependent tangential motion extending over several megaparsecs.

Two independent null tests establish the robustness of this signal. Randomization of filament axes strongly suppresses the measured circulation, demonstrating that the effect is geometrically aligned with filament orientations rather than arising from isotropic velocity fluctuations or estimator bias. Relocation of filament segments to distant environments likewise suppresses the signal, indicating that filament-scale circulation depends on the surrounding large-scale velocity field rather than on filament geometry alone.

A key phenomenological result is selectivity. While many filaments are consistent with null circulation, a subset exhibits coherent, filament-aligned rotation with amplitudes lying well outside both geometry-destroying and environment-destroying null envelopes. This behavior demonstrates that filament-scale Eulerian rotation is not a universal property of the cosmic web but instead reflects specific dynamical conditions.

The analysis is intentionally model-agnostic. No assumptions are made regarding the physical origin of the observed circulation, nor are connections drawn to particular theories of structure formation or angular momentum acquisition. The results presented here therefore establish filament-scale Eulerian circulation as a reproducible observational phenomenon, characterized by coherence, selectivity, and environmental dependence.

These findings motivate future work to characterize the spatial distribution and distance dependence of the signal, to compare across independent velocity reconstructions and simulations, and to investigate possible physical mechanisms. The present study provides a reproducible, field-based empirical foundation for such investigations.

References

Sandrine Codis, Dmitri Pogosyan, Christophe Pichon, and et al. Connecting the cosmic web to the spin of dark haloes. *Monthly Notices of the Royal Astronomical Society*, 448:3391–3404, 2015. doi: 10.1093/mnras/stv245.

Thierry Sousbie. The persistent cosmic web and its filamentary structure. *Monthly Notices of the Royal Astronomical Society*, 414:350–383, 2011. doi: 10.1111/j.1365-2966.2011.18430.x.

M. Tudorache, G. Jung, M. Jarvis, et al. Evidence for coherent rotation in cosmic filaments. *Monthly Notices of the Royal Astronomical Society*, 2025. Accepted.

R. Brent Tully, Hélène Courtois, Romain Graziani, Yehuda Hoffman, and Jenny G. Sorce. Cosmicflows-4. *Astrophysical Journal Supplement Series*, 146(4):86, 2023. doi: 10.3847/1538-4365/acd4f8.

Simon D. M. White. Angular momentum growth in protogalaxies. *Astrophysical Journal*, 286:38–41, 1984. doi: 10.1086/162573.